Effect of Clay on Properties of Ionic Thermoplastic Elastomer Based on EPDM

THOMAS KURIAN,[1] P. P. DE,[1] D. K. TRIPATHY,[1] S. K. DE,[1,*] and D. G. PEIFFER[2]

[1]Rubber Technology Centre, Indian Institute of Technology, Kharagpur 721302, India, and [2]Exxon Research & Engineering Company, Route 22 East, Clinton Township, New Jersey 08801

SYNOPSIS

Incorporation of hard clay causes improvement in most of the physical properties of zinc-sulfonated EPDM of high ethylene content. Zinc stearate reduces the melt viscosity of the clay-filled zinc-sulfonated EPDM during high-temperature processing, but does not adversely affect the physical properties at ambient temperatures. Studies include the measurement of physical properties, scanning electron microscopy (SEM), processability studies in a Monsanto processability tester (MPT), and dynamic mechanical analyses (DMA). © 1996 John Wiley & Sons, Inc.

INTRODUCTION

Ionomers are polymers containing low levels of ionic groups.[1] The biphasic structure of ionomers arises due to the occurrence of a hard phase in the vicinity of ionic groups in the chains, which act as physical crosslinks. Ionomers have emerged as industrial polymers, because of their improved physical properties.[2] Zinc-sulfonated EPDM of high ethylene content (75 wt %), hereafter abbreviated as SEPDM, has the unique ability to behave as a crosslinked elastomer at ambient temperatures and to undergo melt-flow behavior at elevated temperatures as with thermoplastics. It functions as a thermoplastic elastomer and thus could be processed by thermoplastic processing techniques.[3] Although reinforcing fillers are known to adversely affect the properties of thermoplastic elastomers, it has been reported earlier that carbon black and precipitated silica act as reinforcing agents in the case of SEPDM.[3] Incorporation of zinc stearate in SEPDM causes reduction in the melt viscosity, thus facilitating processing of the polymer.[4] The objective of the present work was to study the effect of clay on the physical properties of SEPDM and the role of zinc stearate as an ionic plasticizer in the clay-filled SEPDM compound.

* To whom correspondence should be addressed.

Journal of Applied Polymer Science, Vol. 62, 1729–1734 (1996)
 CCC 0021-8995/96/101729-06

EXPERIMENTAL

Materials

Polymers used in this study are (1) EPDM (M_n, 52,000; M_w, 151,000) containing 75% ethylene, 20% propylene, and 5% 5-ethylidine-2-norbornene and (2) SEPDM (level of sulfonation, 30 meq/100 g polymer) formed by the sulfonation of the pendant unsaturation in the above EPDM, followed by neutralization of the resultant EPDM sulfonic acid using the procedure described by Makowski et al.[5] Both polymers were supplied by Exxon Research & Engineering Co., New Jersey. The hard clay used was Clayfil Grade 1, manufactured by English Indian Clays Ltd., Trivandrum, and its characteristics were as follows: specific gravity, 2.6; minimum fineness through 325 mesh, 99.5%; heat loss (2 h at 105°C), 1% max.; and pH, 4.75. The zinc stearate (melting point, 129°C) used was of rubber grade obtained locally.

Sample Preparation

Rubber compounds were prepared in a Brabender Plasticorder (Model PLE-330) using a cam-type rotor. Mixing was done for 6 min at a rotor speed of 80 rpm and at a temperature of 150°C. The unfilled polymers were also masticated under the same conditions. Test specimens were prepared by molding

Table I Physical Properties at 25°C

Property	Composition of the Mix					
	EPDM	SEPDM	SEPDM + Clay 10 phr	SEPDM + Clay 20 phr	SEPDM + Clay 35 phr	SEPDM + Clay 35 phr + Zinc Stearate 10 phr
Hardness (Shore A)	56	69	70	76	79	79
Modulus at 300% elongation (MPa)	2.7	7.3	8.1	9.0	9.7	9.8
Tensile strength (MPa)	11.0	23.0	22.8	21.2	21.0	20.8
Elongation at break (%)	1036	691	644	621	513	541
Tear strength (kNm^{-1})	63	115	146	171	191	179
Abrasion loss ($cm^3\ h^{-1}$)	0.29	0.21	0.14	0.11	0.08	0.09
Hysteresis loss ($Jm^{-2}\ 10^3$)	82	146	219	268	319	330

in an electrically heated hydraulic press for 5 min at 160°C under a pressure of 10 MPa.

Determination of Physical Properties

Hardness was determined as per ASTM D2240 (1986) and expressed in Shore A units. The stress–strain properties were determined at 25°C according to ASTM D412 (1987) using dumbbell specimens in a Zwick universal testing machine (UTM), Model 1445, using a cross-head speed of 500 mm/min. The tear resistance was determined as per ASTM D624 (1986) using unnicked 90° angle test pieces (die C) at 25°C at a cross-head speed of 500 mm/min in a Zwick UTM Model 1445. The abrasion resistance was determined in a DuPont abrasion tester (BS 903: Part A9 1957 method C) and expressed as abrasion loss, which is the volume in cm^3 abraded from a test specimen per hour. The hysteresis loss was determined under a strain mode according to ASTM D412 (1980) by stretching dumbbell specimens to a strain level of 200% in a Zwick UTM Model 1445.

Scanning Electron Microscopy

The tear-fractured surfaces were sputter-coated with gold within 24 h of testing and examined under a Cam Scan series 2DV scanning electron microscope (SEM).

Determination of Processability

The processability studies were carried out using a Monsanto Processability Tester (MPT) at a temperature of 190°C with the shear rates of 36, 90, 181, and 289 s^{-1}. The capillary length (29.77 mm)-to-diameter (1.50 mm) ratio was 20 with a compound entrance angle of 45° and 60°. The preheat time for each sample was 5 min.

Dynamic Mechanical Analysis

Dynamic mechanical properties were measured in a Rheovibron DDV-III-EP viscoelastometer at a frequency of 3.5 Hz and a strain amplitude of 0.0025 cm. The measurements were carried out over a temperature range of −100 to +200°C at a heating rate of 1°C/min.

RESULTS AND DISCUSSION

Physical Properties

The physical properties of the unfilled polymers and the SEPDM compounds are summarized in Table I. The hardness of SEPDM was higher than that of EPDM. Hardness is a measure of the modulus of elasticity at low strain.[6] The higher hardness of SEPDM could be attributed to the presence of ionic aggregates.[7] The hardness of SEPDM was found to increase as the clay loading increased. There was no change in the hardness of the clay-filled SEPDM compound on addition of zinc stearate.

SEPDM showed a higher modulus and tensile strength and lower elongation at break as compared to EPDM due to the presence of ionic domains which act as physical crosslinks.[8] Incorporation of clay caused a gradual increase in modulus and decrease

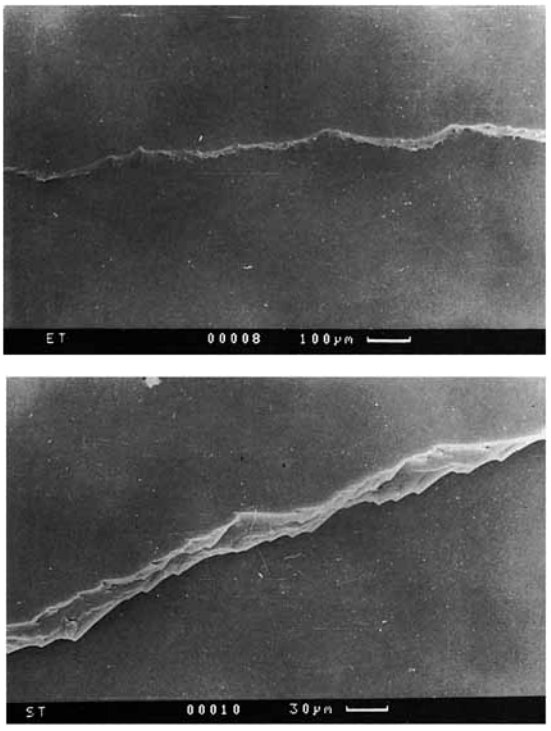

Figure 1 Scanning electron photomicrographs of (a) tear-fractured surface of EPDM and (b) tear-fractured surface of SEPDM.

in elongation at break of SEPDM, but the tensile strength remained almost constant. Although zinc stearate increased the elongation at break of the clay-filled SEPDM compound, the modulus and tensile strength remained unaltered.

SEPDM showed higher tear strength and abrasion resistance as compared to the control EPDM. Figure 1 shows the scanning electron photomicrographs of the tear-fractured surfaces of unfilled EPDM and SEPDM. The fractograph of EPDM [Fig. 1(a)] exhibits a single straight tear line, which propagates from one end to other in a stick-slip manner. The occurrence of a straight tear path in a smooth surface is an indication of low tear strength.[9] SEPDM, on the other hand, shows multiple tear lines propagating in a stick-slip manner [Fig. 1(b)]. This may be due to the deviation of tear path caused by the ionic aggregates[10] and accounts for a twofold increase in tear strength of SEPDM, as compared to EPDM. The gradual increase in tear strength of SEPDM in the presence of clay suggests possible reinforcement of the matrix. Incorporation of clay caused a gradual reduction in the abrasion loss of SEPDM. The higher abrasion resistance of SEPDM and its clay-filled compounds could be attributed to the higher strength of the matrix, as evident from their higher modulus compared to EPDM.[11] Zinc stearate reduced the tear resistance. The abrasion loss of the clay-filled SEPDM compound remained almost unchanged in the presence of zinc stearate.

The results of hysteresis studies are shown in Figure 2. The hysteresis shown by SEPDM could be attributed to the additional energy-dissipation mechanisms also arising out of the ionic aggregates. The ionic aggregates may be considered to behave as ultrafine particles of a reinforcing filler in addition to acting as multifunctional crosslinks.[7,10] The gradual increase in hysteresis of SEPDM on addition of clay (Table I) suggests additional energy-dissipation mechanisms, such as the motion of filler particles, chain slippage, or breakage and dewetting at high strains.[10] The results suggest that clay reinforces SEPDM as discussed later in this article. Zinc stearate marginally increased the hysteresis of the clay-filled SEPDM compound.

Processability

The log–log plots of apparent viscosity vs. shear rate are shown in Figure 3. At all shear rates, SEPDM showed a higher viscosity than that of EPDM. The viscosity of SEPDM increased on addition of clay. The melt viscosity of the clay-filled SEPDM containing zinc stearate was lower than that of unfilled SEPDM. It was reported earlier that zinc stearate plasticizes the ionic aggregates by a solvation mechanism.[1,4,12]

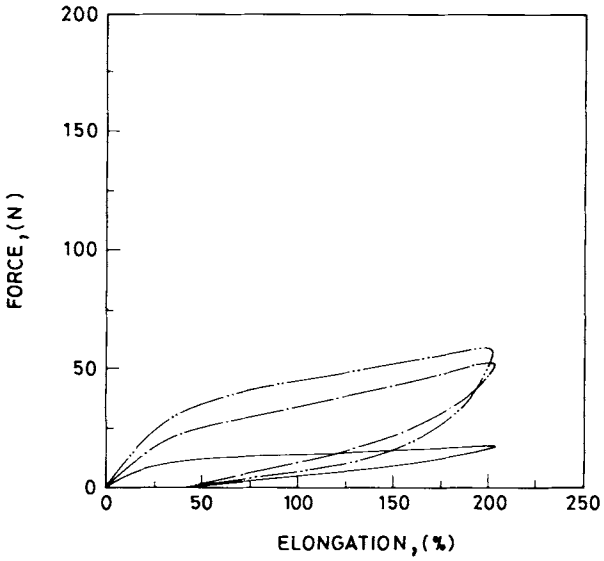

Figure 2 Hysteresis plots at 25°C of (———) EPDM, (——·——) SEPDM, and (——··——) SEPDM + clay 35 phr.

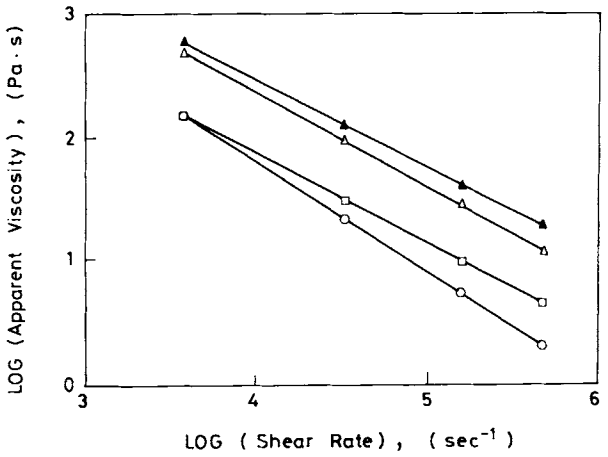

Figure 3 Apparent viscosity vs. shear rate at 170°C of (-○——○-) EPDM, (-△——△-) SEPDM, (-▲——▲-) SEPDM + clay 35 phr, and (-□——□-) SEPDM + clay 35 phr + zinc stearate 10 phr.

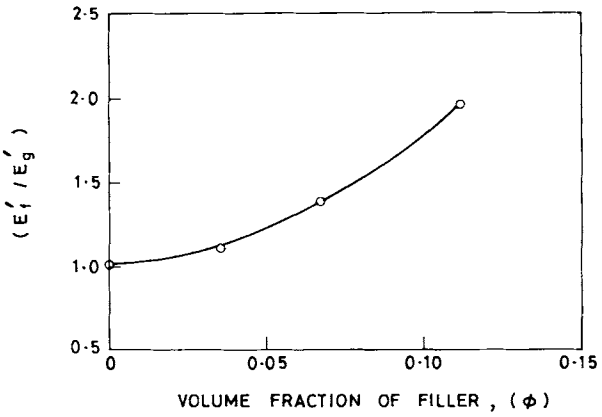

Figure 4 Effect of volume fraction of clay on the relative storage modulus of SEPDM.

Dynamic Mechanical Properties

The results of dynamic mechanical analyses are summarized in Table II. SEPDM showed a higher storage modulus than that of EPDM. Incorporation of clay increased the storage modulus of SEPDM. Reinforcement of SEPDM by clay is evident from the plot of E'_f/E'_g vs. the volume fraction of the filler (ϕ) (Fig. 4) which could be represented by the relation

$$E'_f/E'_g = 1 + 1.2\phi + 65\phi^2 \quad (1)$$

where E'_f is the storage modulus of the filled compound, and E'_g, the storage modulus of the unfilled SEPDM at 25°C. Zinc stearate increased the storage modulus of clay-filled SEPDM at room temperature.

Figure 5 shows the plot of loss tangent vs. temperature obtained from the dynamic mechanical analyses of unfilled polymers and the SEPDM compounds. The glass–rubber transition (T_g) occurs around −26°C in the case of EPDM and SEPDM. Incorporation of clay caused a slight increase in the T_g (from −26 to −23°C) due to stiffening of backbone chains. Incorporation of zinc stearate did not alter the T_g of the clay-filled SEPDM. The tan δ_{max} (i.e., the tan δ value at T_g) was less in the case of SEPDM as compared to EPDM because of the stiffening imparted by ionic domains in SEPDM.[13] Incorporation of clay caused a lowering of the tan δ_{max} of SEPDM due to possible rubber–filler interaction involving the backbone chains.[14] Zinc stearate caused a further decrease in the tan δ_{max} due to the stiffening of the chains at low temperature.

Figure 6 shows the plot of $(\tan \delta_{max})_f/(\tan \delta_{max})_g$ vs. the volume fraction of the filler (ϕ). Here, f stands

Table II Results of Dynamic Mechanical Analyses

Composition of the Mix	T_g[a] (°C)	tan δ at T_g (tan δ_{max})	Transition Due to Ionic Aggregates[b] (T_i, °C)	tan δ at T_i	Transition Due to Melting of Crystallities[b] (°C)	Storage Modulus (E') at 25°C (MPa)
EPDM	−26	0.365	—	—	[c]	11.0
SEPDM	−26	0.257	+27 to +80	0.040	+119	19.8
SEPDM + clay 10 phr	−24	0.255	+27 to +62	0.050	+120	21.7
SEPDM + clay 20 phr	−23	0.253	+27 to +62	0.054	+120	27.4
SEPDM + clay 35 phr	−23	0.249	+27 to +58	0.054	+120	38.4
SEPDM + clay 35 phr + zinc stearate 10 phr	−22	0.214	+27 to +62	0.067	+105	54.3

[a] From $(\tan \delta)_{max}$ in the plot of tan δ vs. temperature.
[b] From tan δ vs. temperature plot.
[c] Not detectable.

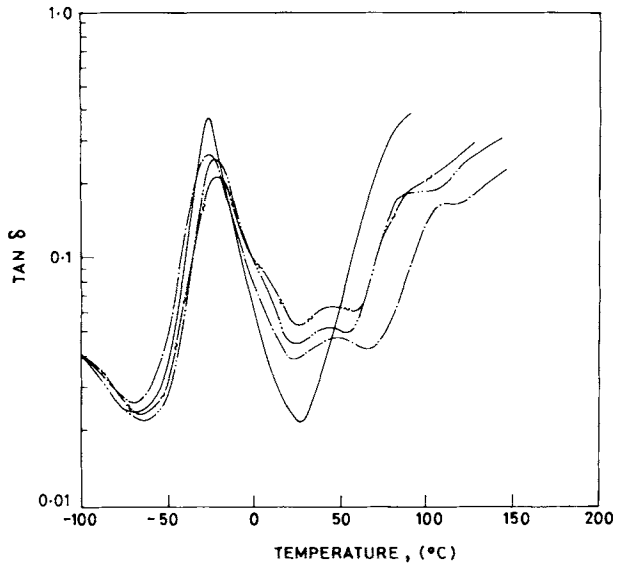

Figure 5 Semilogarithmic plots of tan δ vs. temperature of (———) EPDM, (— · —) SEPDM, (— · · —) SEPDM + clay 35 phr, and (—~—) SEPDM + clay 35 phr + zinc stearate 10 phr.

for the filled system and g denotes the unfilled SEPDM. The results could be fitted into the following relation:

$$(\tan \delta_{max})_f/(\tan \delta_{max})_g = 1 - 0.17\phi - 1.1\phi^2 \quad (2)$$

The nature of the plot indicates rubber–filler interaction.[15]

Apart from the T_g, SEPDM and its compounds showed two other transitions: one around 119°C, which is believed to be due to the melting of the crystalline zone of the polyethylene block, and another broad transition observed as a broad plateau

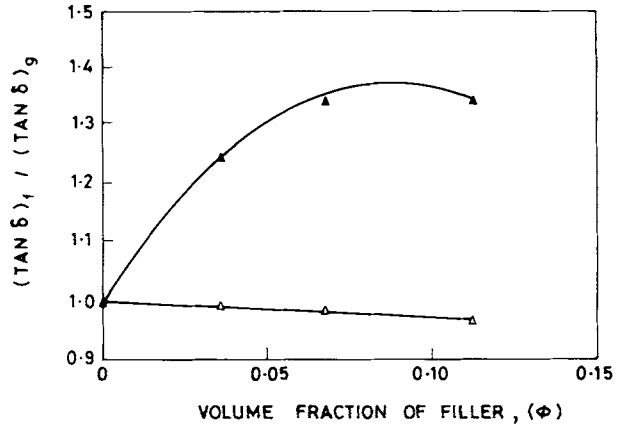

Figure 6 Effect of volume fraction of clay on the relative tan δ value of SEPDM (△) at T_g and (▲) at T_i.

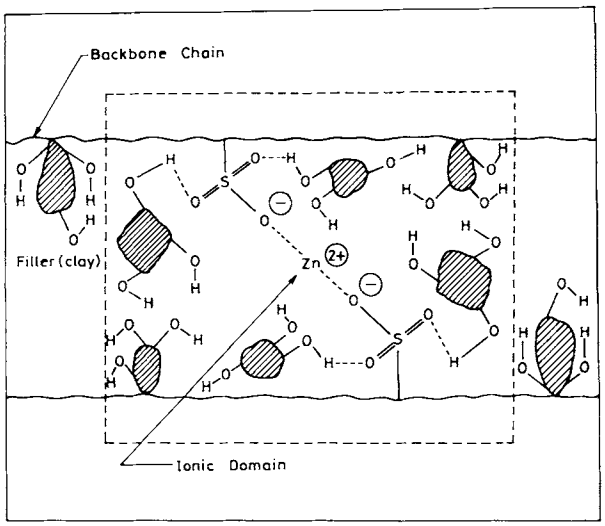

Figure 7 Proposed schematic representation of the attachment of clay particles to the backbone chains and the interaction between hydroxyl groups of clay and ionic aggregates of SEPDM.

in the temperature range of +27 to +80°C which is ascribed to the transition of a hard phase arising out of the ionic aggregates.[3] A transition due to the ionic aggregates was found to occur in a similar temperature range in the case of rubbery ionomers.[1,16] In the case of crystalline ionomers, a transition due to ionic aggregates has been reported to occur at a temperature lower than the crystalline melting temperature.[17–19] Incorporation of clay reduced the breadth of the plateau at the ionic transition region, the corresponding temperature being designated as T_i, and increased the height of the plateau region (i.e., tan δ at T_i). Incorporation of zinc stearate caused a further increase in tan δ at T_i, but the breadth remained almost similar. While the reason

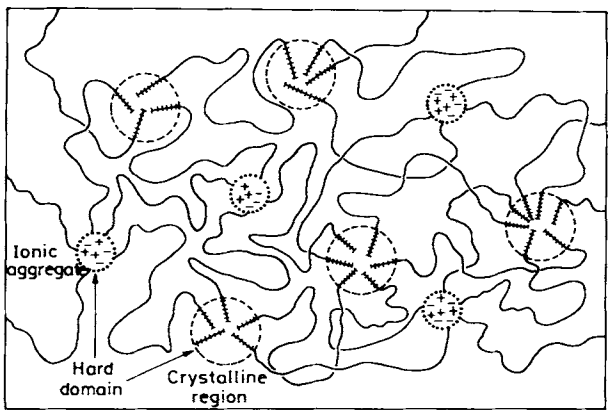

Figure 8 Proposed schematic morphological structure of SEPDM containing 75 wt % ethylene.

for the changes in the breadth of the plateau region is not understood, an increase in tan δ at T_i is ascribed to the strengthening of the hard phase, which is responsible for the high-temperature transition of the ionomer.[3]

Figure 6 shows the variation of $(\tan \delta)_f/(\tan \delta)_g$ at T_i versus the volume fraction of the filler (ϕ). The results obey the following relationship:

$$(\tan \delta)_f/(\tan \delta)_g = 1 + 8.5\phi - 48.9\phi^2 \quad (3)$$

From the above results, it could be inferred that the rubber–filler interaction in the case of the clay-filled SEPDM is of two types: (1) the interaction between the filler particles and the nonpolar polymer backbone of SEPDM, which is similar to the interaction involving diene rubbers and reinforcing fillers, as manifested in the increase in storage modulus and lowering of tan δ at the T_g and (2) the interaction between the ionic groups of the polymer and the polar groups (—OH) present on the surface of the filler particles, which is manifested in an increase in tan δ at T_i. While the rubber–filler interaction involving the nonpolar polymer backbone is of a weak van der Waals type, the same involving ionic aggregates might be stronger as proposed in Figure 7.

In the case of EPDM, expectedly, the broad transition due the ionic aggregates was not observed and the high-temperature transition due to the crystalline melting zone could not be detected because of the softening of the sample above 100°C. However, the presence of ionic aggregates in SEPDM makes the matrix rigid enough for the crystalline melting zone to be detected. The morphological structure of SEPDM is believed to be similar to that of conventional thermoplastic elastomers, i.e., a combination of hard domains and soft segments as proposed in Figure 8. While the crystallites due to polyethylene blocks and ionic aggregates due to metal sulfonate groups may constitute the hard domains, the EPDM backbone may act as soft segments.

CONCLUSIONS

Hard clay improves the physical properties of SEPDM. Zinc stearate acts as a plasticizer under processing conditions and as a low reinforcing filler under ambient conditions. Dynamic mechanical analyses show the occurrence of a biphasic structure in SEPDM and its clay-filled compounds. Both a main-chain glass–rubber transition in the low-temperature region and the high-temperature ionic transition are influenced by the incorporation of clay.

REFERENCES

1. P. K. Agarwal, H. S. Makowski, and R. D. Lundberg, *Macromolecules,* **13,** 1679 (1980).
2. W. J. MacKnight and R. D. Lundberg, *Rubb. Chem. Technol.,* **57,** 652 (1984).
3. T. Kurian, D. Khastgir, P. P. De, D. K. Tripathy, S. K. De, and D. G. Peiffer, *Polymer,* **36,** 3875 (1995).
4. T. Kurian, A. K. Bhattacharya, P. P. De, D. K. Tripathy, S. K. De, and D. G. Peiffer, *Plast. Rubb. Compos. Process. Appl.,* **24,** 285 (1995).
5. H. S. Makowski, R. D. Lundberg, and J. Bock, U.S. Pat. 4,184,988 (1980) (to Exxon Research and Engineering Co.).
6. T. H. Ferrigno, in *Handbook of Fillers and Reinforcements for Plastics,* H. S. Katz and J. V. Milewski, Eds., Van Nostrand Reinhold, New York, 1978.
7. B. Hird and A. Eisenberg, *Macromolecules,* **25,** 6466 (1992).
8. A. Eisenberg and M. King, in *Ion Containing Polymers,* Academic Press, New York, 1977.
9. N. M. Mathew and S. K. De, *Polymer,* **23,** 632 (1982).
10. A. I. Medalia and G. Kraus, in *Science and Technology of Rubbers,* F. R. Eirich, Ed., Academic Press, New York, 1994.
11. B. Kuriakose and S. K. De, *J. Mater. Sci.,* **20,** 1864 (1985).
12. U. K. Mondal, D. K. Tripathy, and S. K. De, *Polym. Eng. Sci.,* **36,** 283 (1996).
13. P. P. A. Smit, *Rheol. Acta,* **5,** 277 (1966).
14. N. K. Datta and D. K. Tripathy, *J. Appl. Polym. Sci.,* **44,** 1635 (1992).
15. D. Roy, A. K. Bhowmick, and S. K. De, *Polym. Eng. Sci.,* **32,** 971 (1992).
16. U. K. Mondal, D. K. Tripathy, and S. K. De, *Polymer,* **34,** 3832 (1993).
17. S. Yano, N. Nagao, M. Hattori, E. Hirasawa, and K. Tadano, *Macromolecules,* **25,** 368 (1992).
18. S. Yano, K. Tadano, N. Nagao, S. Kutsumizu, H. Tachino, and E. Hirasawa, *Macromolecules,* **25,** 7168 (1992).
19. W. J. MacKnight, L. W. McKenna, and B. E. Read, *J. Appl. Phys.,* **38,** 4208 (1967).

Received January 29, 1996
Accepted June 1, 1996